BIOCELL
2023 47(11): 2485-2494

Tech Science Press

# Inhibition of VEGF-A expression in hypoxia-exposed fetal retinal microvascular endothelial cells by exosomes derived from human umbilical cord mesenchymal stem cells

Jing LI[1,2]; Wanwan FAN[4]; Lili HAO[1]; Yongsheng LI[5]; Guocheng YU[1]; Wei SUN[6]; Xianqiong LUO[2,*]; Jingxiang ZHONG[1,3,*]

[1] Department of Ophthalmology, The First Affiliated Hospital of Jinan University, Jinan University, Guangzhou, 510630, China
[2] Department of Ophthalmology, Guangdong Women and Children Hospital, Guangzhou, 511400, China
[3] Department of Ophthalmology, The Sixth Affiliated Hospital of Jinan University, Jinan University, Dongguan, 523000, China
[4] Graduate School, Guangzhou Medical University, Guangzhou, 510000, China
[5] Lab Center, Guangdong Cord Blood Bank, Guangzhou, 510000, China
[6] Guangdong Eye Institute, Department of Ophthalmology, Guangdong Provincial People's Hospital (Guangdong Academy of Medical Sciences), Southern Medical University, Guangzhou, 510000, China

**Key words:** Mesenchymal stem cells, Exosomes, Immature fetal retinal vascular endothelial cells, Vascular endothelial growth factor A, Hypoxia

**Abstract: Objective:** This study aimed to investigate the potential of human umbilical cord mesenchymal stem cell (hucMSC)-derived exosomes (hucMSC-Exos) in inhibiting hypoxia-induced cell hyper proliferation and overexpression of vascular endothelial growth factor A (VEGF-A) in immature human fetal retinal microvascular endothelial cells (hfRMECs). **Methods:** Exosomes were isolated from hucMSCs using cryogenic ultracentrifugation and characterized through various techniques, including transmission electron microscopy, nanoparticle tracking analysis, bicinchoninic acid assays, and western blotting. The hfRMECs were identified using von Willebrand factor (vWF) co-staining and divided into four groups: a control group cultured under normoxic condition, a hypoxic model group, a hypoxic group treated with low-concentration hucMSC-Exos (75 μg/mL) and a hypoxic group treated with high-concentration hucMSC-Exos (100 μg/mL). Cell viability and proliferation were assessed using Cell Counting Kit-8 (CCK-8) assay and EdU (5-ethynyl-2′-deoxyuridine) assay respectively. Expression levels of VEGF-A were evaluated using RT-PCR, western blotting and immunofluorescence. **Results:** Hypoxia significantly increased hfRMECs' viability and proliferation by upregulating VEGF-A levels. The administration of hucMSC-Exos effectively reversed this response, with the high-concentration group exhibiting greater efficacy compared to the low-concentration group. **Conclusion:** In conclusion, hucMSC-Exos can dose-dependently inhibit hypoxia-induced hyperproliferation and VEGF-A overexpression in immature fetal retinal microvascular endothelial cells.

**Abbreviations**

| | |
|---|---|
| **hucMSC** | human umbilical cord mesenchymal stem cell |
| **hucMSC-Exos** | hucMSCs-derived exosomes |
| **VEGF-A** | vascular endothelial growth factor A |
| **hfRMEC** | human fetal retinal microvascular endothelial cell |
| **vWF** | von Willebrand factor |
| **ROP** | retinopathy of prematurity |
| **EC** | vascular endothelial cell |
| **OIR** | oxygen-induced retinopathy |
| **HIF-1** | hypoxia-inducible factor-1 |
| **HIMF** | hypoxia-induced mitogenic factor |

## Introduction

Retinopathy of prematurity (ROP) is a vaso-proliferative retinal disease that leads to visual impairment and blindness in premature infants and low birth weight babies. In normally developing human fetus, retinal vascular development begins around gestational week 16 and progresses from the center towards the peripheral retina until full-term. Consequently, premature infants exhibit areas of incomplete peripheral retinal vascularization. The

*Address correspondence to: Jingxiang Zhong, zjx85221206@126.com; Xianqiong Luo, luoxqgz@126.com
Received: 23 July 2023; Accepted: 16 October 2023;
Published: 27 November 2023

Doi: 10.32604/biocell.2023.044177 

elevated levels of oxygen tension (hyperoxia) experienced after birth, in comparison to their prenatal exposure, hinder the production and secretion of proangiogenic factors. Consequently, this exacerbates the apoptosis of vascular endothelial cells (ECs) during the initial vaso-obliteration phase of ROP. Subsequently, the retina encounters hypoxic due to its heightened oxygen demand for maturation, thus initiating the second vaso-proliferative phase. Hypoxia triggers a compensatory release of extensive angiogenic factors promoting neovascularization. Ultimately, these leaky vessels lead to intravitreal hemorrhages, fibrovascular membranes, retinal detachment and eventual blindness (Dai *et al.*, 2021).

Among all angiogenic factors, VEGF emerges as a key player in the pathogenesis of ROP. Thus, targeting VEGF has garnered considerable attention as a therapeutic approach for ROP. Experimental evidence indicates that the downregulation of VEGF can lead to a significant reduction in the neovascular response while facilitating the development of normal retinal vessels, thereby improving the peripheral avascular retina. Several subsequent multicenter trials have unveiled numerous advantages associated with anti-VEGF intravitreal injections compared to traditional laser therapy for ROP treatment. These benefits include a shorter treatment administration time, more rapid disease improvement and ROP regression, reduced visual field defects and a lower risk of refractive errors (Mintz-Hittner *et al.*, 2016; Stahl *et al.*, 2019). Currently, ranibizumab and bevacizumab (the latter being used off-label) represent the most frequently employed anti-VEGF medications. It has been reported that due to the limited half-life of these medications (2.5 to 3 days), ROP frequently experiences recurrences, requiring repeated injections, and consequently, demanding frequent and prolonged ocular surveillance (Lyu *et al.*, 2017). Another concern arises from the potential systemic adverse effects on the physiological process of normal angiogenesis in the developing organs of preterm infants due to the decrease in serum VEGF levels following the administration of intravitreal anti-VEGF agents (Fidler *et al.*, 2020; Sato *et al.*, 2012).

Over the past decade, there has been rapid advancement in cell-based therapeutics. These treatments offer two significant advantages compared with traditional drug therapy: long-term efficacy and excellent biocompatibility. In the oxygen-induced retinopathy (OIR) mice model, a well-established animal model of ROP, intravitreally injected mesenchymal stem cells (MSCs) derived from bone marrow and human placental amniotic membrane demonstrated beneficial vascular effects by reducing the avascular area and neovascularization (Kim *et al.*, 2016; Xu *et al.*, 2020). MSCs, characterized as multipotent progenitor cells, can be obtained from various tissue sources, including bone marrow, adipose tissue, dental-origin samples, placenta, peripheral blood, umbilical cord tissue and umbilical cord blood. Human umbilical cord mesenchymal stem cells (hucMSCs) emerge as a preferable choice for clinical applications when compared to MSCs from other sources. This preference arises from their inherent advantages, including easier and noninvasive collection methods, reduced ethical concerns, enhanced differentiation capacity, accelerated self-renewal capabilities and lower immunogenicity (Chia *et al.*, 2021; Li *et al.*, 2015).

Paracrine mechanisms, mainly mediated by cell-free exosomes derived from MSCs, cell-free exosomes, underlie the therapeutic effects of MSCs (Mosquera *et al.*, 2021). Exosomes, nano-sized extracellular vesicles secreted by cells, possess the same functions as their parental cells (Desrochers *et al.*, 2016). Exosome-based therapies can address safety concerns associated with MSC transplantation, including issues such as integration deficiency, vitreous opacification, retinal detachment, allogeneic immunological rejection, vascular occlusion, reactive gliosis and retinal degeneration (Li *et al.*, 2016; Tassoni *et al.*, 2015). Both ranibizumab and bevacizumab have been reported to inhibit the retinal vascularization of ROP infants, primarily because they lack of precise cellular targeting (Sukgen *et al.*, 2016). Exosomes selectively transfer crucial bioactive cargos to specific cells by virtue of their surface molecules, thereby presenting the possibility of preventing avascular areas (Wu *et al.*, 2023).

According to previous studies, the intravitreal injection of hucMSCs and hucMSC-Exos appears to represent a viable therapeutic strategy for various retinal diseases, including macular holes, age-related macular degeneration, diabetic retinopathy and retinal laser damage (Fu *et al.*, 2021; Yu *et al.*, 2016; Zhang *et al.*, 2018). However, to date, no experiments have been conducted in either *in vitro* or *in vivo* ROP models. VEGF, which is the major pathogenic factor in ROP, has been reported to be suppressed by hucMSC-Exos in blue light-injured human retinal pigment epithelial cells and laser-induced choroidal neovascularization. This suggests that hucMSC-Exos exert their protective effects through the regulation of VEGF (He *et al.*, 2018). Additionally, in breast tumors, Lee *et al.* (2013) demonstrated that hucMSC-Exos could inhibit angiogenesis by suppressing the expression of VEGF.

In the current study, we established a hypoxic model using hfRMECs and hypothesized that hucMSC-Exos could effectively target VEGF-A. To test this hypothesis, we conducted a series of experiments, including cell viability and proliferation assays, western blotting, quantitative polymerase chain reaction and immunofluorescence analysis.

## Materials and Methods

The group designs and schematic experiment protocol are presented as Fig. 1.

### *Isolation and identification of hucMSC-Exos*

Fresh umbilical cord tissues were obtained from a puerpera at Guangdong Women and Children Hospital after obtaining informed consent. Primary hucMSCs were isolated as previously described (Qiao *et al.*, 2008). Briefly, penicillin–streptomycin (Leagene, Beijing, China) was added to phosphate-buffered solution (PBS) for a 15 min wash of the umbilical cord tissues. After removing the arteries and veins, the umbilical cord tissues were cut into small approximately 3 mm * 3 mm blocks. Subsequently, these small tissue blocks were affixed to the bottom of a petri dish and

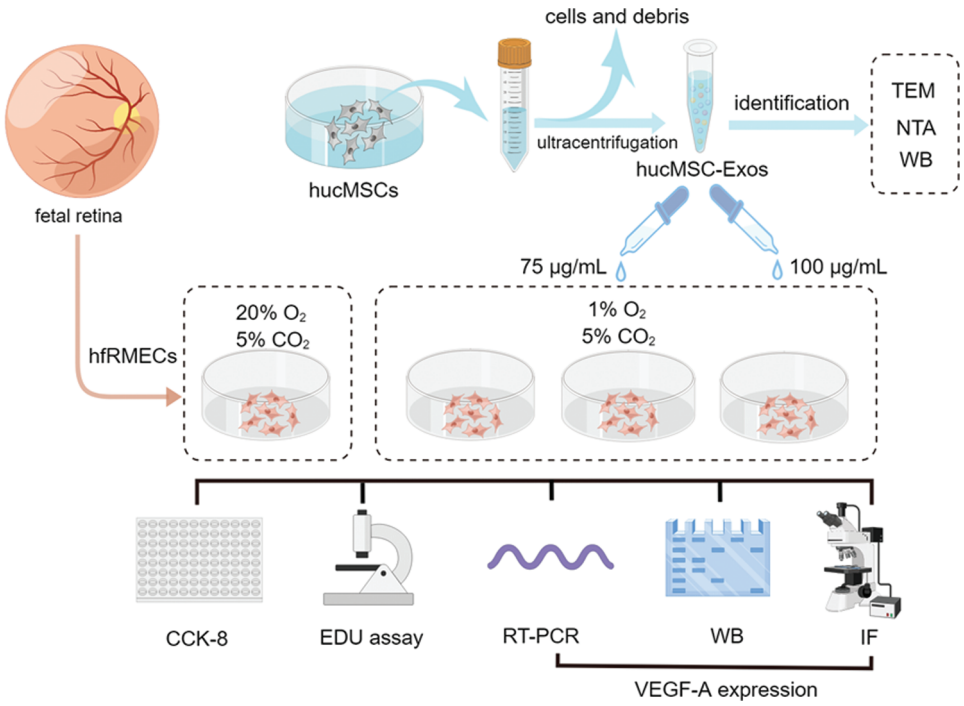


**FIGURE 1.** Schematic protocol (by Figdraw). Schematic representation of the isolation process of hucMSC-Exos and *in vitro* experiments involve in hfRMECs.

incubated for 60 min in a cell culture incubator. The culture medium, which contained α-MEM (Invitrogen, Cal, USA), 20% FBS (Bovogen, Melbourne, Australia) and penicillin–streptomycin, was replaced every 3 days. Fibroblastic colonies developed around the tissue 12–14 days later. The flow cytometric characteristic of hucMSCs was assessed by labelling with standard surface markers, including CD 90, CD 105, CD 73, CD 34 and CD 45 (San Jose, CA, USA) and fluorescence was detected using Cytoflex flow cytometry (BD, San Jose, USA).

hucMSCs from passage 4 were used for exosome collection. The conditioned medium was collected and centrifuged at 2,000 × g for 30 min and 10,000 × g for 45 min to remove cells and debris when hucMSCs reached 50% confluence. Subsequently, the samples were purified with a 0.45 μm fiber membrane and clarified supernatant liquid was centrifuged twice at 100,000 × g for 70 min each time and immediately diluted with PBS. Finally, the hucMSC-Exos were stored at −80°C. Their morphology, size and protein concentration were determined using transmission electron microscopy (TEM; Tecnai G2 Spirit, FEI, Hillsboro, United USA), nanoparticle tracking analysis (NTA; NS300, Malvern, UK) and BCA assay (Pierce, Rockford, USA). Surface marker antibodies CD 9 (ImmunoWay, Texas, USA), CD 63 (ImmunoWay, Texas, USA) and Alix (Santa Cruz, CA, USA) were identified by western blotting.

*Isolation, culture and treatment of hfRMECs*

ECs were derived from the eyes of a spontaneously aborted fetus donated by a puerpera after obtaining informed consent at Guangdong Women and Children Hospital. The procedures for harvesting ECs have been previously described (Li *et al.*, 2008). Briefly, we anatomically separated the neural retina through cutting the eyes circumferentially posterior to the limbus, and removing other segments including cornea, lens, vitreous, sclera and retinal pigment epithelium. The neural retinas were then further sectioned into smaller fragments and subjected to a 2.5% trypsin (HyClone, Logan, USA) digestion at 37°C for 30 min. The homogenate was concentrated by centrifugation at 1,000 × g for 10 min and subjected to an additional 30-min digestion in 1.33% collagenase. After another round of centrifugation at 1,000 × g for 10 min, the pellet was resuspended in conditioned medium, which consisted of human serum-free endothelial-basal growth medium (Invitrogen, Carlsbad, USA) with 50 U/mL endothelial cell growth factor and 20% fetal bovine serum (Sigma-Aldrich, St. Louis, USA). Following seeding in fibronectin-coated dishes, the cells were incubated in a humidified atmosphere containing 5% $CO_2$ at 37°C. The cultured cells were characterized for endothelial homogeneity by detecting intracellular expression of von Willebrand factor (vWF, Abcam, Cambridge, UK) by immunofluorescence analysis.

hfRMECs in passages 3 to 6 were utilized in this study and were randomly allocated to four groups as follows: 1. hfRMECs cultured under normoxia (20% $O_2$, 5% $CO_2$) with no treatment (marked as Ctrl); 2. hfRMECs exposed to hypoxia (1% $O_2$, 5% $CO_2$) with no treatment (marked as Hypoxia); 3. Hypoxic hfRMECs pretreated with 75 μg/mL hucMSC-Exos for 24 h (marked as Hypoxia+L-Exo); 4. Hypoxic hfRMECs pretreated with 100 μg/mL hucMSC-Exos for 24 h (marked as Hypoxia+H-Exo). The hypoxic condition was applied in a humidified incubation chamber at 37°C.

*Exosome labeling and internalization*

PKH67, a lipophilic dye, was used to label hucMSC-Exos (BBoxiProbe, Nanjing, China). In brief, hucMSC-Exos were incubated with a mixture of PKH67 and Diluent C for 12 h at 4°C. Following removal of the medium and resuspension in PBS, exosomes were concentrated via ultracentrifugation in the dark at 100,000 × g for 90 min twice at 4°C.

For the cell uptake assay, hfRMECs were seeded in 24-well plates and incubated with 20 ug/mL PKH67 labeled exosomes at 37°C for 24 h. Then, the cells were washed with PBS and fixed in 4% paraformaldehyde (Beyotime, Shanghai, China) for 15 min. The nucleis were counterstained with 4′,6-diamidino-2-phenylindole (DAPI; Solarbio, Beijing, China). Images were sequentially acquired with an inverted fluorescence microscope (Mshot#MF52, Guangzhou, China).

*CCK-8 assay and proliferation assay*

Cell viability was assessed using a Cell Counting Kit-8 (CCK-8; Beyotime, Shanghai, China). Briefly, hfRMECs from different groups were seeded in 96-well plates ($5 \times 10^3$ per well) and cultured overnight. After subjecting hucMSC-Exos to either normoxia or hypoxia for 24 h, we introduced a mixture consisting of CCK-8 reagent and DMEM (1:10) into the cell culture medium (100 μl per well) and incubated it for 1.5 h at 37°C. Subsequently, the absorbance was measured at 450 nm using a microplate reader (Tecan F50, Mannedorf, Switzerland).

To evaluate cell proliferation capacity of different groups, BeyoClick™ EdU Cell Proliferation Kit with Alexa Fluor 488 (Beyotime, Shanghai, China) was used. Briefly, hfRMECs were inoculated into 48-well plates overnight and incubated with EdU solution (10 μM) for 4 h. Following fixation with 4% paraformaldehyde, cells underwent a 30-min incubation with the click reaction solution in the absence of light. Finally, the nucleis were counterstained with Hoechst 33342 (Beyotime, Shanghai, China). Images were captured using an inverted fluorescence microscope. The percentage of EdU-positive cells, defined as the number of EdU-positive cells (green) divided by the total cell count (blue), was calculated in nine random microscopic fields.

*Immunofluorescence analysis*

For immunofluorescence staining, hfRMECs plated in chamber slides were initially fixed with cold acetone for 10 min and subsequently permeabilized with PBS containing 0.1% Triton X-100 (BioFroxx, Einhausen, German) and 1% BSA for 5 min. Afterward, they were blocked with PBS containing 1% BSA for 1 h at RT, the samples were incubated with VEGF-A primary antibody (rabbit polyclonal, 1:200, Proteintech, Wuhan, China) at 4°C overnight, followed by secondary antibodies (Goat anti-Rabbit IgG/FITC, 1:200, Solarbio, Beijing, China) for 1.5 h at RT. Following thorough washing, the samples were incubated with DAPI (Solarbio, Beijing, China) for 5 min at RT. The samples were shielded from light and examined using an inverted fluorescence microscope.

*Quantitative reverse transcription polymerase chain reaction*

Total RNA was isolated from hfRMECs using TRIzol reagent (Invitrogen, Carlsbad, USA) according to the manufacturer's instructions. A DNase I Kit (Sigma–Aldrich, St. Louis, USA) was used to remove any genomic DNA and the treated RNA was then converted to cDNA using PrimeScript® RT Master Mix (TaKaRa, Shiga, Japan). The oligonucleotide primers used for PCR were VEGF-A, 5′-GAGGGCAGAATCATCACGAAG-3′ (sense) and 5′-TGTGCTGTAGGAAGCTCATCTCTC-3′ (antisense); β-actin, 5′-CGTCACCAACTGGGACGA-3′ (sense) and 5′-ATGGGGGAGGGCATACC-3' (antisense). The target genes were amplified on a LightCycler®96 Real-Time PCR System (Roche, Basel, Switzerland) with SYBR® Premix Ex TaqTM (Beyotime, Shanghai, China). Relative expression of mRNA was calculated using the comparative $2^{-\Delta\Delta Ct}$ method as described (Livak and Schmittgen, 2001). The copy numbers of VEGF-A were first normalized to those of 18S mRNA and then to those of the control group.

*Western blotting analysis*

For Western blotting analysis, hfRMECs were collected, washed and lysed with RIPA cell lysis buffer (Beyotime, Shanghai, China). The lysates were homogenized on ice for 20 min and centrifuged at 12,000 × g for 10 min. Protein concentration in the supernatant was determined using a BCA protein assay kit (Beyotime, Shanghai, China) and adjusted to a final concentration of 2 μg/μl. Following the addition of 5× loading buffer, the protein samples were boiled at 98°C for 5 min.

Protein samples (20 μg) were separated by 12% sodium-dodecyl sulfate-PAGE and then transferred to a polyvinylidene fluoride membrane (Roche, Basel, Switzerland). The membranes were blocked with 5% nonfat milk at RT for 1 h and then incubated at 4°C overnight with primary antibodies (VEGF-A, Rabbit polyclonal, 1:1,000, Proteintech, Wuhan, China; β-actin, Rabbit polyclonal, 1:10,000, Abcam, Cambridge, UK). After being washed with PBST for three times (10 min per time), the membranes were incubated with horseradish peroxidase–conjugated goat anti-rabbit IgG (1:20,000, HuaAn, Hangzhou, China) for 1 h. Visualization was performed using an ultrasensitive ECL chemiluminescence kit (BeyoECL Star, Beyotime, Shanghai, China). For quantitative comparison, band intensities were analyzed using Image J software, first normalized to β-actin, and then further normalized to the control group.

*Statistical analysis*

All the results presented are representative of at least three separate experiments. Data are presented as the mean ± SD. All parameters were compared by ANOVA followed by *post hoc* Newman–Keuls analysis with significance defined at $p < 0.05$.

## Results

*Identification of hucMSCs and hucMSC-Exos*

Typical spindle shapes were displayed by the P4 passage hucMSCs (Fig. 2A). Flow cytometric analysis confirmed the positive staining of hucMSCs for CD 90, CD 105 and CD 73, while negative for CD 34 and CD 45, as illustrated in Fig. 2B. hucMSC-Exos were successfully isolated using the ultracentrifugation method. As shown in Fig. 2C, the exosomes were cup-shaped with a visible bilayer membrane structure on the periphery and low electron density components in the interior of the cavity. The western blotting results showed that hucMSC-Exos expressed typical exosomal markers CD 9, CD 63 and Alix, indicating successful isolation of exosomes (Fig. 2D). NTA technology showed that the

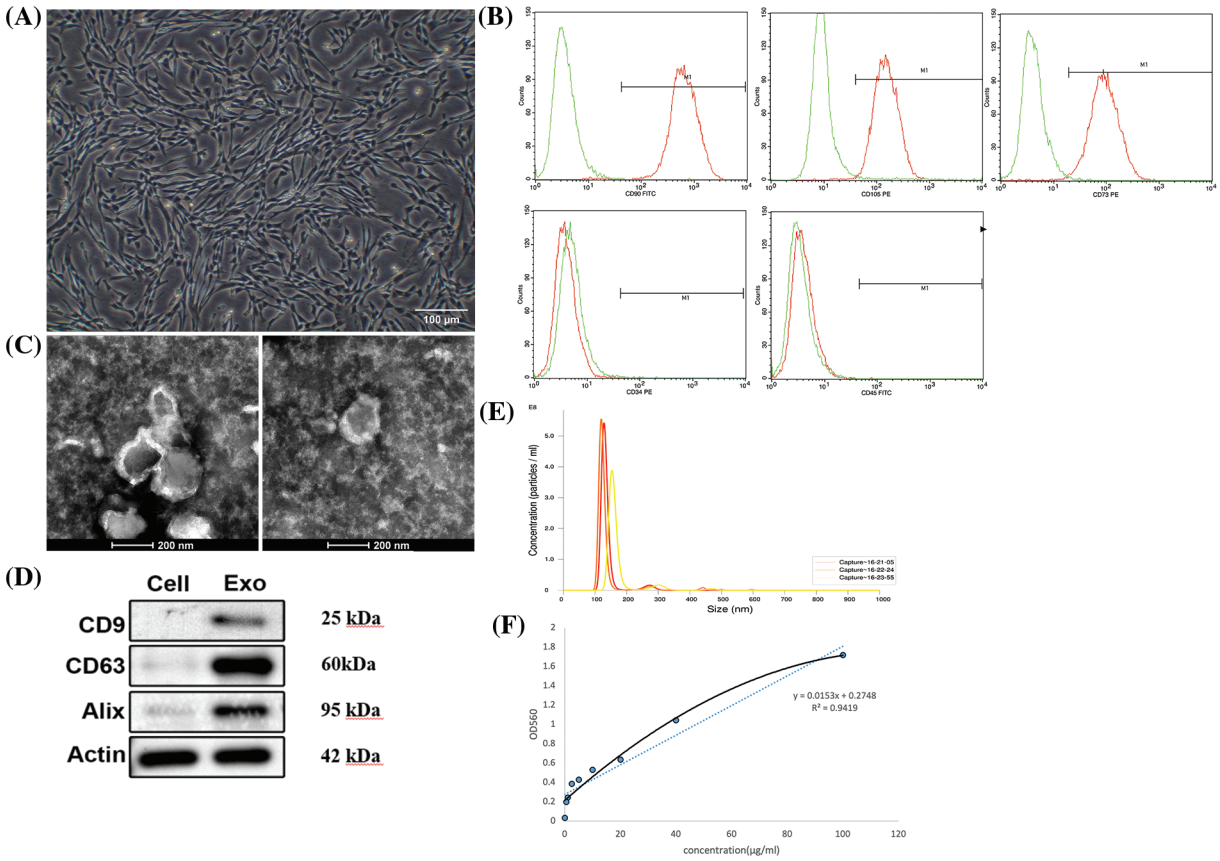


**FIGURE 2.** Identification and characterization of hucMSC-Exos. (A) The morphology of P4 hucMSCs under a microscope. Scale bar: 100 μm. (B) Flow cytometry results for expression of stem cell surface markers CD 90, CD 105, CD 73, CD 34 and CD 45. (C) The ultrastructure of hucMSC-Exos under TEM. Scale bar: 200 nm. (D) The expression of CD 9, CD 63 and Alix in hucMSC-Exos identified by Western blotting with the lysates of hucMSCs serving as control. (E) NTA of hucMSC-Exos. (F) The standard curve of BCA assay.

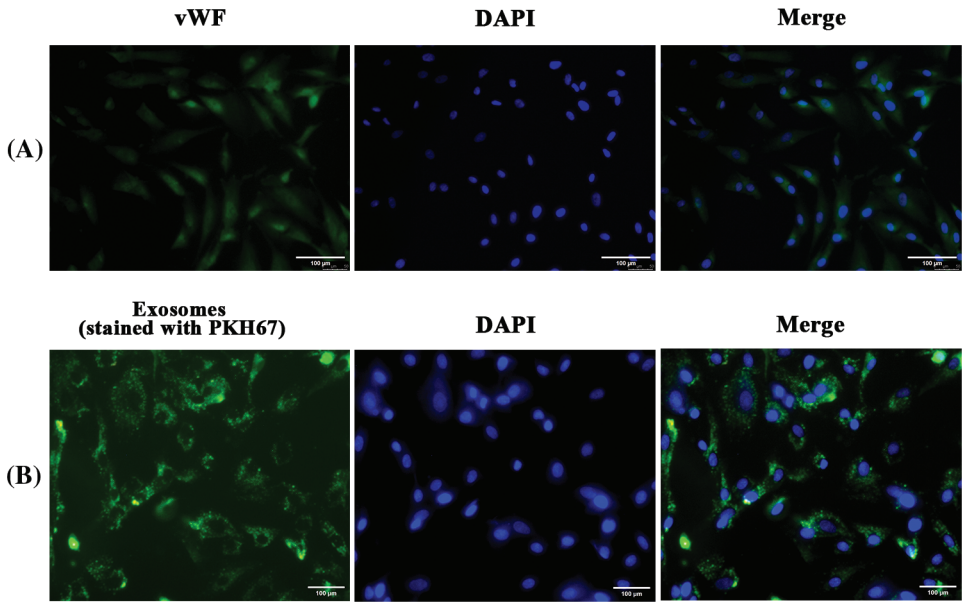


**FIGURE 3.** (A) Immunofluorescence staining of hfRMECs with vWF (green). Scale bar: 100 μm. (B) PKH67 (green)-labeled hucMSC-Exos were taken up by hfRMECs. Scale bar: 100 μm.

particle size of the hucMSC-Exos ranged from 120 to 160 nm with an average of 148.1 ± 11.8 nm (Fig. 2E). The BCA method showed that the protein concentration of hucMSC-Exos was 12.38 ± 0.86 mg/mL (Fig. 2F).

*hfRMECs identification and hucMSC-Exos internalization*

hfRMECs were identified by immunofluorescence staining with the EC-specific marker vWF (Fig. 3A). Previous study showed that MSCs derived extracellular vesicles were

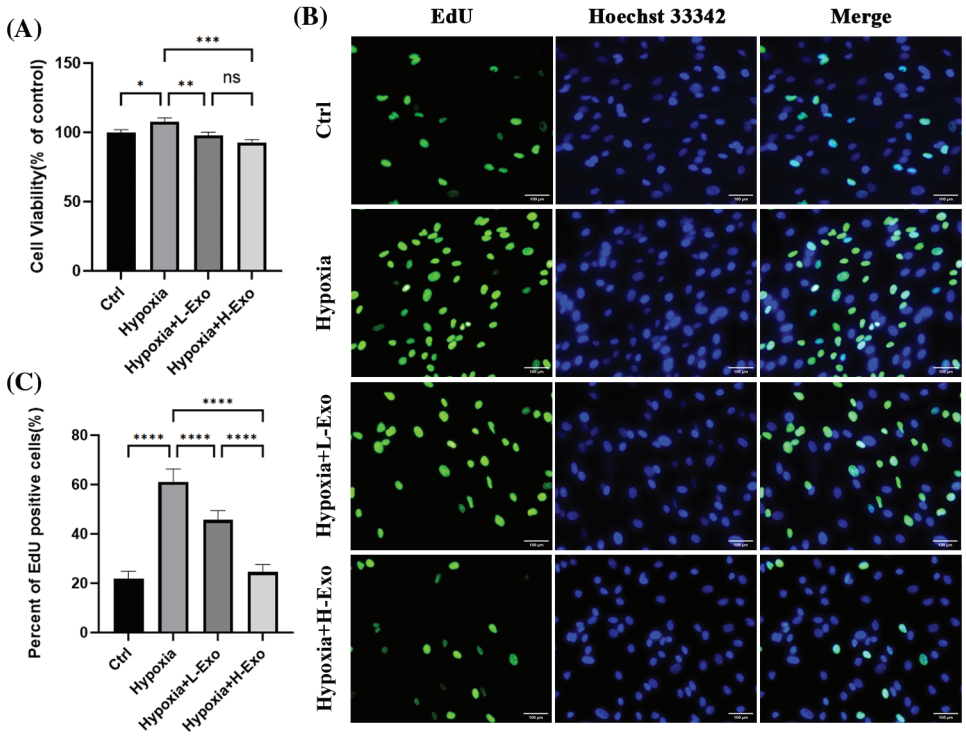


**FIGURE 4.** Effects of hucMSC-Exos in the hfRMECs under hypoxic conditions. (A) CCK-8 assay for cell viability of hfRMECs. (B) The EdU assay for cell proliferation of hfRMECs showed positive cells in green fluorescence. Scale bar: 100 μm. (C) The percentage of EdU-positive cells. Data are shown as mean ± SD. n = 3. *$p < 0.05$, **$p < 0.01$, ***$p < 0.001$, ****$p < 0.0001$, ns: no significance (Ctrl: hfRMECs under normoxia, Hypoxia: hfRMECs under hypoxia, Hypoxia+L-Exo: Hypoxic hfRMECs pretreated with 75 μg/mL hucMSC-Exos, Hypoxia+H-Exo: Hypoxic hfRMECs pretreated with 100 μg/mL hucMSC-Exos).

detected 2 h after treatment in ECs and accumulated over time. Oxidative stress has no effect on the capacity of ECs to uptake the vesicles (Xiao *et al.*, 2021). In the present study, we added PKH67-labeled hucMSC-Exos (green) to hfRMECs culture medium at a final concentration of 20 ug/mL, and green fluorescence was widely distributed in the cytoplasm of most hfRMECs 24 h later (Fig. 3B).

*hucMSC-Exos suppressed the viability and proliferation of hfRMECs*

The viability and proliferation rate of the hfRMECs exposed to hypoxia significantly increased compared to those cultured in normoxic condition. However, this trend was effectively reversed by hucMSC-Exos. After co-culture with hucMSC-Exos for 24 h, the viability and proliferation rate of hfRMECs decreased significantly compared to the hypoxic hfRMECs without intervention (Figs. 4A–4C). The higher concentration of hucMSC-Exos at 100 μg/mL exhibited a more pronounced inhibitory effect on proliferation than the lower concentration of 75 μg/mL (Fig. 4C).

*hucMSC-Exos downregulated VEGF-A in hypoxic hfRMECs*

Immunofluorescence results demonstrated that after a 24 h co-culture with hucMSC-Exos, hypoxic hfRMECs showed reduced intracellular VEGF-A levels. The degree of downregulation appeared to be somewhat proportional to the intervention concentrations (Fig. 5A). The relative levels among each group were significantly different (Fig. 5B). The level of VEGF-A mRNA substantially increased in the hypoxic group and markedly decreased upon the addition of hucMSC-Exos. Notably, the extent of downregulation of VEGF-A mRNA levels appeared to correlate with the concentration of hucMSC-Exos administered (Fig. 5C). To further quantify this reaction, we measured VEGF-A protein by using western blotting. Under hypoxic conditions, VEGF-A protein level increased up to nearly twofold compared to those of the normoxic group and were decreased by the intervention of hucMSC-Exos. After coculture with hucMSC-Exos at a concentration of 100 μg/mL, the levels returned to basal values. However, the high concentration group showed no greater effect in downregulating VEGF-A protein level compared to the low concentration group (Figs. 5D and 5E).

## Discussion

It is recognized that MSCs secrete extracellular vesicles to facilitate intercellular communication. Regarding their biogenesis, extracellular vesicles can be categorized into three main types: microvesicles (200–2,000 nm), apoptotic bodies (500–2,000 nm) and exosomes (40–200 nm) (Shao *et al.*, 2018). The process of exosome formation involves several stages, including the initiation of endosome formation through inward budding of the cell membrane, subsequent endosome maturation, and the incorporation of transmembrane proteins, cytosolic contents, and peripheral proteins. Different types of surface proteins can be found on exosomes generated from varied sources, along with RNA, DNA, intracellular proteins, amino acids and metabolites. Previous studies have indicated the enrichment of

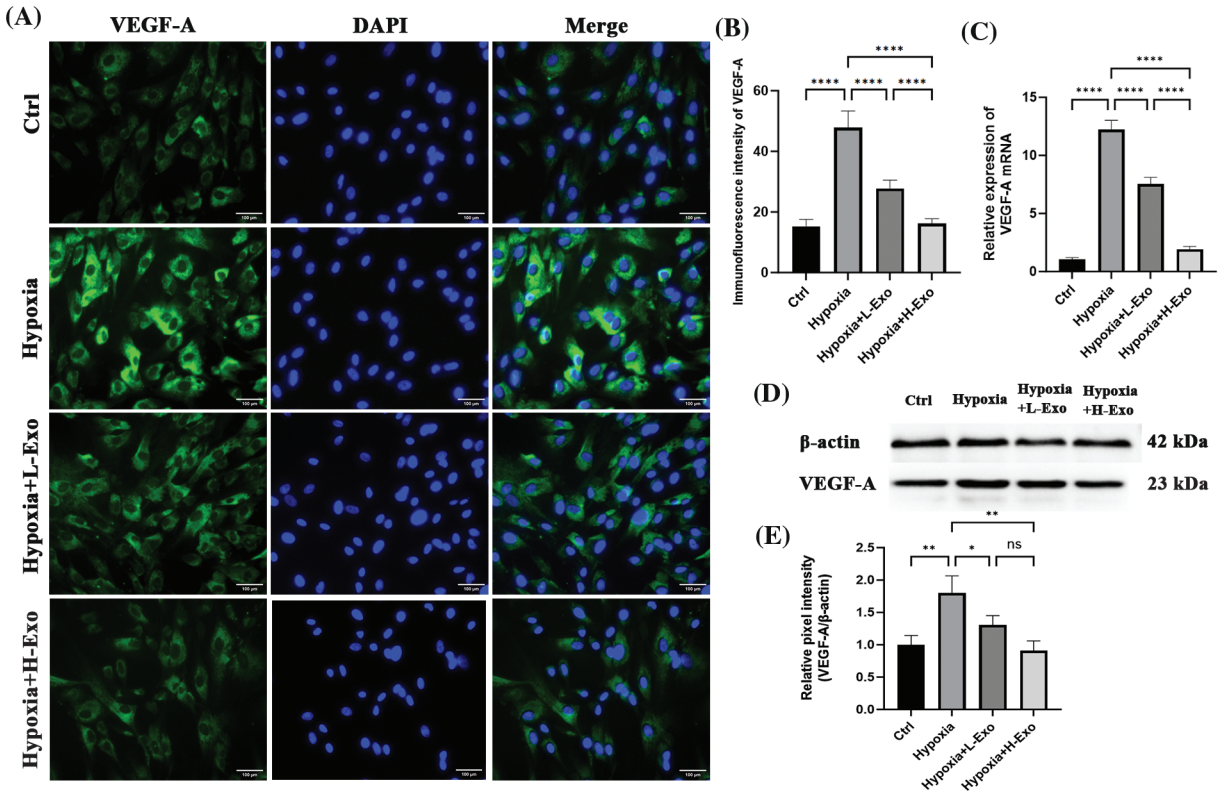


**FIGURE 5.** The levels of VEGF-A decreased consistently with increasing concentrations of hucMSC-Exos. (A) Immunofluorescence staining showed positive staining of VEGF-A (green) in hfRMECs. DAPI was used to stain the nucleis (blue). Scale bar: 100 μm. (B) The relative immunofluorescence densities were quantified using bar graphs. (C) RT-PCR results for VEGF-A mRNA levels. (D) The expression of VEGF-A protein in hfRMECs was determined using western blotting. (E) Relative band densities of VEGF-A. Data are shown as mean ± SD. n = 3. *$p < 0.05$, **$p < 0.01$, ***$p < 0.001$, ****$p < 0.0001$. ns: no significance (Ctrl: hfRMECs under normoxia, Hypoxia: hfRMECs under hypoxia, Hypoxia+L-Exo: Hypoxic hfRMECs pretreated with 75 μg/mL hucMSC-Exos, Hypoxia+H-Exo: Hypoxic hfRMECs pretreated with 100 μg/mL hucMSC-Exos).

transmembrane lipid-bound proteins such as CD 9, CD 63 and Alix in hucMSC-Exos (Xiao *et al.*, 2021).

Human fetal tissue provides a practical alternative source of retinal microvascular endothelial cells from multiple donors. In this study, we successfully cultured retinal microvascular endothelial cells from a spontaneously aborted fetus and the cells stained positive for the endothelial marker vWF. Subsequently, we used a hypoxic hfRMECs model to investigate the impact of hucMSC-Exos. Given the inherent heterogeneity of immature fetal endothelial cells in both physiological and pathological contexts compared to their mature adult counterparts (Andrews *et al.*, 2018), our study has established a validated *in vitro* model that more accurately replicates the pathogenesis of ROP in preterm infants. Biochemical hypoxia and atmospheric hypoxia are major methods to generate hypoxic conditions. In the former approach, oxygen deprivation conditions induced by chemical compounds can modulate hypoxia-related signaling but are unable to replicate the hypoxia-mediated mitochondrial ROS signaling (Stenger *et al.*, 2011). Therefore, we selected the latter method, in which hypoxia is induced by replacing oxygen molecules with nitrogen in a controlled gas mixture within an airtight chamber.

In the present study, hfRMECs exhibited obvious hyperproliferation and increased expression levels of the key angiogenesis-related protein VEGF in response to hypoxia, consistent with the findings reported by Mammadzada *et al.* (2016). Subsequent investigations confirmed the inhibitory effect of hucMSC-Exos on hypoxic hfRMECs, aligning with the outcomes of a study by Guang-Hui He, which demonstrated significant reduction of VEGF-A expression in human retinal vascular endothelial cells exposed to high glucose in a time- and concentration-dependent manner (He *et al.*, 2021). However, the molecular mechanism by which hucMSC-Exos prevent VEGF production remains unclear.

Hypoxia-inducible factor-1 (HIF-1), a nuclear transcription factor directly governing the release of various growth factors, including VEGF, angiopoietin, and erythropoietin, is crucial for neovascularization and cell proliferation. Growing evidence implicated HIF-1 as a significant participant in the pathological process of ROP (Swan *et al.*, 2018). Recently studies have suggested that hucMSC-Exos may inhibit cell proliferation and vascular remodeling via suppression of hypoxia-induced mitogenic factor (HIMF), a critical upstream mediator of HIF-1 signaling (Lee *et al.*, 2012). Consequently, we hypothesized that anti-VEGF effect of hucMSC-Exos observed in this study may be mediated through the inhibition of HIMF-HIF-1-VEGF signaling pathway. However, future research is warranted to provide concrete evidence of hucMSC-Exos

directly inhibit expression of HIF-1α and alleviate retinal neovascularization *in vitro* and *in vivo*.

Exosomes are known to transport a substantial cargo of active messenger RNAs (mRNAs), microRNAs (miRNAs) and proteins, influencing cell and organ functions in a targeted manner. It is recognized that miRNAs encapsulated in MSC-Exos are key functional molecules responsible for certain beneficial effects. miRNAs are nonprotein coding RNA molecules that can influence gene expression by affecting transcription, translation and epigenetics. Multiple miRNAs have been identified and confirmed to regulate angiogenesis by recent studies. Several experimental and clinical studies have investigated the relationship between miRNAs, VEGF and ROP. Some miRNAs could target mRNAs regulating VEGF expression, and some could directly target VEGF through receptors and signaling pathways. Zhao *et al.* (2014) analyzed the expression change of retinal miRNAs in an OIR rat model and found that a total of 66 miRNAs, of which VEGF was listed among the target genes, were affected during the process of oxygen-induced retinal neovascularization. van *et al.* (2012) identified an increase in retinal vascularization and VEGF levels as miR-214 expression decreased, indicating that miRNA-214 targets the mRNA of VEGF at the gene level. In RMECs exposed to high glucose, miR-146 was identified to suppress VEGF levels via the STAT3 pathway and inhibit apoptosis via IL-6 signaling (Ye and Steinle, 2017). Nunes *et al.* (2015) showed a decrease in a series of microRNAs, including miR-17, miR-20, miR-93 and miR-106 in the *in vivo* ROP mouse model of angiogenesis and identified miR-17 family members as the key molecules in early steps of neovascularization. Metin *et al.* (2018) performed the first clinical study. These researchers detected a significant decrease in miR-27b, miR-214 and miR-29a expression in premature infants with ROP compared with controls. Since miR-27b is known to suppress angiogenesis via inhibition of VEGF-C in cancer tissue, its upregulation in the retina may also inhibit retinal neovascularization by downregulating VEGF, suggesting a potential therapeutic effect for ROP. Jothimani *et al.* (2022) confirmed that the miRNAs mentioned above, including miR-146, miR-27, miR-17, miR-214, miR-20 and miR-106, were abundantly found in hucMSC-Exos. It has been revealed that miR-20 can directly target the 3'UTR region of VEGF-A mRNA and that miR-17 can regulate VEGF by targeting HIF-1 (Zhang *et al.*, 2022). Consequently, the addition of hucMSC-Exos to hypoxic hfRMECs led to the downregulation of VEGF in our present study.

## Conclusion

Considerable interest has been sparked in exosome-based therapies. In this study we isolated and identified exosomes from hucMSCs. Given the early onset of ROP in infants, the use of human fetal retinas allowed us to work with primary endothelial cells that better recapitulate the pathogenesis of the disease.

Our findings conclusively demonstrated the capacity of hucMSC-Exos to effectively attenuate hypoxia-induced cell hyperproliferation and VEGF-A overexpression in hfRMECs. Although the precise mechanism remains elusive, the observed anti-VEGF biological activity of hucMSC-Exos may offer a promising and innovative approach for the treatment of ROP.

**Acknowledgement:** None.

**Funding Statement:** This study was supported by the following funds: 1. Medical Scientific Research Foundation of Guangdong Province (A2022221); 2. Natural Science Foundation of Guangdong Province (2019A1515011417); 3. National Natural Science Foundation of China (81970806, 82271094); 4. Science and Technology Projects in Guangzhou (202201020030, 202201020015); 5. Guangdong High-Level Hospital Construction Fund (ynkt2021-zz16). The funding body played no role in the design of the study and collection, analysis, and interpretation of data and in writing the manuscript.

**Author Contributions:** The authors confirm contribution to the paper as follows: study conception and design: JL, JXZ and XQL; data collection: WWF, YSL and WS; analysis and interpretation of results: JL, LLH and GCY; draft manuscript preparation: JL; final approval of the manuscript: JXZ. All authors reviewed the results and approved the final version of the manuscript.

**Availability of Data and Materials:** The datasets generated during and/or analyzed during the current study are available from the corresponding author on reasonable request.

**Ethics Approval:** The study was approved by the Ethics Committee of Guangdong Women and Children Hospital (202101220).

**Conflicts of Interest:** The authors declare that they have no conflicts of interest to report regarding the present study.

## References

Andrews AM, Lutton EM, Cannella LA, Reichenbach N, Razmpour R, Seasock MJ, Kaspim SJ, Merkel SF, Langford D, Persidsky Y et al. (2018). Characterization of human fetal brain endothelial cells reveals barrier properties suitable for in vitro modeling of the BBB with syngenic co-cultures. *Journal of Cerebral Blood Flow and Metabolism* **38**: 888–903. https://doi.org/10.1177/0271678X17708690

Chia WK, Cheah FC, Aziz NHA, Kampan NC, Wong YP (2021). A review of placenta and umbilical cord-derived stem cells and the immunomodulatory basis of their therapeutic potential in bronchopulmonary dysplasia. *Frontiers in Pediatrics* **9**: 615508. https://doi.org/10.3389/fped.2021.615508

Dai C, Webste KA, Bhatt A, Tian H, Su GF, Li W (2021). Concurrent physiological and pathological angiogenesis in retinopathy of prematurity and emerging therapies. *International Journal of Molecular Sciences* **22**: 4809. https://doi.org/10.3390/ijms22094809

Desrochers LM, Antonyak MA, Cerione RA (2016). Extracellular vesicles: Satellites of information transfer in cancer and stem cell biology. *Developmental Cell* **37**: 301–309. https://doi.org/10.1016/j.devcel.2016.04.019

Fidler M, Fleck BW, Stahl A, Marlow N, Chastain JE, Li J, Lepore D, Reynolds JD, Chiang MF, Fielder AR (2020). Ranibizumab population pharmacokinetics and free VEGF pharmacodynamics in preterm infants with retinopathy of prematurity in the RAINBOW trial. *Translational Vision Science & Technology* **9**: 43. https://doi.org/10.1167/tvst.9.8.43

Fu Y, He GH, Chen S, Gu ZH, Zhang YL, Li LY (2021). Protective effects of umbilical cord mesenchymal stem cell exosomes in a diabetic rat model through live retinal imaging. *International Journal of Ophthalmology* **14**: 1828–1833. https://doi.org/10.18240/ijo.2021.12.04

He GH, Dong M, Chen S, Wang YC, Gao X, Wu B, Wang J, Wang JH (2021). Mesenchymal stem cell-derived exosomes inhibit the VEGF-A expression in human retinal vascular endothelial cells induced by high glucose. *International Journal of Ophthalmology* **14**: 1820–1827. https://doi.org/10.18240/ijo.2021.12.03

He GH, Zhang W, Ma YX, Yang J, Chen L, Song J, Chen S (2018). Mesenchymal stem cells-derived exosomes ameliorate blue light stimulation in retinal pigment epithelium cells and retinal laser injury by VEGF-dependent mechanism. *International Journal of Ophthalmology* **11**: 559–566. https://doi.org/10.18240/ijo.2018.04.04

Jothimani G, Pathak S, Dutta S, Duttaroy AK, Banerjee A (2022). A Comprehensive cancer-associated microRNA expression profiling and proteomic analysis of human umbilical cord mesenchymal stem cell-derived exosomes. *Tissue Engineering and Regenerative Medicine* **19**: 1013–1031. https://doi.org/10.1007/s13770-022-00450-8

Kim KS, Park JM, Kong T, Kim C, Bae SH, Kim HW, Moon J (2016). Retinal angiogenesis effects of TGF-β1 and paracrine factors secreted from human placental stem cells in response to a pathological environment. *Cell Transplantation* **25**: 1145–1157. https://doi.org/10.3727/096368915X688263

Lee C, Mitsialis SA, Aslam M, Vitali SH, Vergadi E, Konstantinou G, Sdrimas K, Fernandez-Gonzalez A, Kourembanas S (2012). Exosomes mediate the cytoprotective action of mesenchymal stromal cells on hypoxia-induced pulmonary hypertension. *Circulation* **126**: 2601–2611. https://doi.org/10.1161/CIRCULATIONAHA.112.114173

Lee JK, Park SR, Jung BK, Jeon YK, Lee YS, Kim MK, Kim YG, Jang JY, Kim CW (2013). Exosomes derived from mesenchymal stem cells suppress angiogenesis by down-regulating VEGF expression in breast cancer cells. *PLoS One* **8**: e84256. https://doi.org/10.1371/journal.pone.0084256

Li P, Tian H, Li Z, Wang L, Gao F, Ou Q, Lian C, Li W, Jin C, Zhang J et al. (2016). Subpopulations of bone marrow mesenchymal stem cells exhibit differential effects in delaying retinal degeneration. *Current Molecular Medicine* **16**: 567–581. https://doi.org/10.2174/1566524016666160607090953

Li T, Xia MX, Gao YY, Chen T, Xu Y (2015). Human umbilical cord mesenchymal stem cells: An overview of their potential in cell-based therapy. *Expert Opinion on Biological Therapy* **15**: 1–14. https://doi.org/10.1517/14712598.2015.1051528

Li B, Yin W, Hong X, Shi Y, Wang HS, Lin SF, Tang SB (2008). Remodeling retinal neovascularization by ALK1 gene transfection *in vitro*. *Investigative Ophthalmology & Visual Science* **49**: 4553–4560. https://doi.org/10.1167/iovs.07-0995

Livak KJ, Schmittgen TD (2001). Analysis of relative gene expression data using real-time quantitative PCR and the $2^{-\Delta\Delta C_T}$ Method. *Methods* **25**: 402–408. https://doi.org/10.1006/meth.2001.1262

Lyu J, Zhang Q, Chen CL, Xu Y, Ji XD, Li JK, Huang QJ, Zhao PQ (2017). Recurrence of retinopathy of prematurity after intravitreal ranibizumab monotherapy: Timing and risk factors. *Investigative Ophthalmology & Visual Science* **58**: 1719–1725. https://doi.org/10.1167/iovs.16-20680

Mammadzada P, Gudmundsson J, Kvante A, Andre H (2016). Differential hypoxic response of human choroidal and retinal endothelial cells proposes tissue heterogeneity of ocular angiogenesis. *Acta Ophthalmology* **94**: 805–814. https://doi.org/10.1111/aos.13119

Metin T, Dinc E, Gorur A, Erdogan S, Ertekin S, Sari AA, Tamer L, Celik Y (2018). Evaluation of the plasma microRNA levels in stage 3 premature retinopathy with plus disease: Preliminary study. *Eye* **32**: 415–420. https://doi.org/10.1038/eye.2017.193

Mintz-Hittner HA, Geloneck MM, Chuang AZ (2016). Clinical management of recurrent retinopathy of prematurity after intravitreal bevacizumab monotherapy. *Ophthalmology* **123**: 1845–1855. https://doi.org/10.1016/j.ophtha.2016.04.028

Mosquera HMI, Morales LC, Vidal OM, Barcelo E, Silvera-Redondo C, Velez JI, Garavito-Galofre P (2021). Exosomes: Potential disease biomarkers and new therapeutic targets. *Biomedicines* **9**: 1061. https://doi.org/10.3390/biomedicines9081061

Nunes DN, Dias-Neto E, Cardo-Vila M, Kdwards EJ, Dobroff AS, Giordano RJ, Mandelin J, Brentani HP, Hasselgren C, Yao VJ et al. (2015). Synchronous down-modulation of miR-17 family members is an early causative event in the retinal angiogenic switch. *Proceedings of the National Academy of Sciences of the United States of America* **112**: 3770–3775. https://doi.org/10.1073/pnas.1500008112

Qiao C, Xu W, Zhu W, Hu J, Qian H, Yin Q, Jiang R, Yan Y, Mao F, Yang H et al. (2008). Human mesenchymal stem cells isolated from the umbilical cord. *Cell Biology International* **32**: 8–15. https://doi.org/10.1016/j.cellbi.2007.08.002

Sato T, Wada K, Arahori H, Kuno N, Imoto K, Iwahashi-Shima C, Kusaka S (2012). Serum concentrations of bevacizumab (avastin) and vascular endothelial growth factor in infants with retinopathy of prematurity. *American Journal of Ophthalmology* **153**: 327–333 e1. https://doi.org/10.1016/j.ajo.2011.07.005

Shao H, Im H, Castro CM, Breakefield X, Weissleder R, Lee H (2018). New technologies for analysis of extracellular vesicles. *Chemical Reviews* **118**: 1917–1950. https://doi.org/10.1021/acs.chemrev.7b00534

Stahl A, Lepore D, Fielder A, Fleck B, Reynolds JD, Chiang MF, Li J, Liew M, Maier R, Zhu Q et al. (2019). Ranibizumab versus laser therapy for the treatment of very low birthweight infants with retinopathy of prematurity (RAINBOW): An open-label randomised controlled trial. *The Lancet* **394**: 1551–1559. https://doi.org/10.1016/S0140-6736(19)31344-3

Stenger C, Naves T, Verdier M, Ratinaud MH (2011). The cell death response to the ROS inducer, cobalt chloride, in neuroblastoma cell lines according to p53 status. *International Journal of Oncology* **39**: 601–609. https://doi.org/10.3892/ijo.2011.1083

Sukgen EA, Comez A, Kocluk Y, Cevher S (2016). The process of retinal vascularization after anti-VEGF treatment in retinopathy of prematurity: A comparison study between ranibizumab and bevacizumab. *Ophthalmologica* **236**: 139–147. https://doi.org/10.1159/000449530

Swan R, Kim SJ, Campbell JP, Chan RVP, Sonmez K, Taylor KF, Li X, Chen YI, Rotter JI, Simmons C et al. (2018). The genetics of retinopathy of prematurity: A model for neovascular retinal

disease. *Ophthalmology Retina* **2**: 949–962. https://doi.org/10.1016/j.oret.2018.01.016

Tassoni A, Gutteridge A, Barber AC, Osborne A, Martin KR (2015). Molecular mechanisms mediating retinal reactive gliosis following none marrow mesenchymal stem cell transplantation. *Stem Cells* **33**: 3006–3016. https://doi.org/10.1002/stem.2095

van MA, Grundmann S, Goumans MJ, Lei ZY, Oerleman MI, Jaksani S, Doevendans PA, Sluijter JPG (2012). MicroRNA-214 inhibits angiogenesis by targeting Quaking and reducing angiogenic growth factor release. *Cardiovascular Research* **93**: 655–665. https://doi.org/10.1093/cvr/cvs003

Wu KY, Ahmad H, Lin G, Carbonneau M, Tran SD (2023). Mesenchymal stem cell-derived exosomes in ophthalmology: A comprehensive review. *Pharmaceutics* **15**: 1167. https://doi.org/10.3390/pharmaceutics15041167

Xiao X, Xu M, Yu H, Wang L, Li X, Rak J, Wang S, Zhao RC (2021). Mesenchymal stem cell-derived small extracellular vesicles mitigate oxidative stress-induced senescence in endothelial cells via regulation of miR-146a/Src. *Signal Transduction and Targeted Therapy* **6**: 354. https://doi.org/10.1038/s41392-021-00765-3

Xu W, Cheng W, Cui X, Xu G (2020). Therapeutic effect against retinal neovascularization in a mouse model of oxygen-induced retinopathy: Bone marrow-derived mesenchymal stem cells versus Conbercept. *BMC Ophthalmology* **20**: 1–8. https://doi.org/10.1186/s12886-019-1292-x

Ye EA, Steinle JJ (2017). miR-146a suppresses STAT3/VEGF pathways and reduces apoptosis through IL-6 signaling in primary human retinal microvascular endothelial cells in high glucose conditions. *Vision Research* **139**: 15–22. https://doi.org/10.1016/j.visres.2017.03.009

Yu B, Shao H, Su C, Jiang Y, Chen X, Bai L, Zhang Y, Li Q, Zhang X, Li X (2016). Exosomes derived from MSCs ameliorate retinal laser injury partially by inhibition of MCP-1. *Scientific Reports* **6**: 34562. https://doi.org/10.1038/srep34562

Zhang Y, Li SJ, Jin PS, Shang T, Sun RA, Lu LY, Guo KJ, Liu JP, Tong YJ, Wang JB et al. (2022). Dual functions of microRNA-17 in maintaining cartilage homeostasis and protection against osteoarthritis. *Nature Communications* **13**: 2447. https://doi.org/10.1038/s41467-022-30119-8

Zhang XM, Liu JP, Yu B, Ma FF, Ren XJ, Li XR (2018). Effects of mesenchymal stem cells and their exosomes on the healing of large and refractory macular holes. *Graefes Archive for Clinical & Experimental Ophthalmology* **256**: 2041–2052. https://doi.org/10.1007/s00417-018-4097-3

Zhao R, Qian L, Jiang L (2014). Identification of retinopathy of prematurity related miRNAs in hyperoxia-induced neonatal rats by deep sequencing. *International Journal of Molecular Sciences* **16**: 840–856. https://doi.org/10.3390/ijms16010840